
Efficient non-conjugate Gaussian process factor models for spike count data using polynomial approximations

Stephen L. Keeley
Princeton Neuroscience Institute
Princeton University
Princeton, NJ 08542
skeeley@princeton.edu

David M. Zoltowski
Princeton Neuroscience Institute
Princeton University
Princeton, NJ 08542
zoltowski@princeton.edu

Yiyi Yu
Electrical and Computer Engineering
University of California, Santa Barbara
Santa Barbara, CA 93106
yiyiy@ucsb.edu

Jacob L. Yates
Center for Visual Science
University of Rochester
Rochester, NY 14627
jyates7@ur.rochester.edu

Spencer L. Smith
Electrical and Computer Engineering
University of California, Santa Barbara
Santa Barbara, CA 93106
sls@ucsb.edu

Jonathan W. Pillow
Princeton Neuroscience Institute
Princeton University
Princeton, NJ 08542
pillow@princeton.edu

Abstract

Gaussian Process Factor Analysis (GPFA) has been broadly applied to the problem of identifying smooth, low-dimensional temporal structure underlying large-scale neural recordings. However, spike trains are non-Gaussian, which motivates combining GPFA with discrete observation models for binned spike count data. The drawback to this approach is that GPFA priors are not conjugate to count model likelihoods, which makes inference challenging. Here we address this obstacle by introducing a fast, approximate inference method for non-conjugate GPFA models. Our approach uses orthogonal second-order polynomials to approximate the nonlinear terms in the non-conjugate log-likelihood, resulting in a method we refer to as *polynomial approximate log-likelihood* (PAL) estimators. This approximation allows for accurate closed-form evaluation of marginal likelihood and fast numerical optimization for parameters and hyperparameters. We derive PAL estimators for GPFA models with binomial, Poisson, and negative binomial observations, and additionally show that the parameters obtained can be used to initialize black-box variational inference, which significantly speeds up and stabilizes the inference procedure for these factor analytic models. We apply these methods to data from mouse visual cortex and monkey higher-order visual and parietal cortices, and compare GPFA under three different spike count observation models to traditional GPFA. We demonstrate that PAL estimators achieve fast and accurate extraction of latent structure from multi-neuron spike train data.

1 Introduction

Recent advances in neural recording technologies have enabled the collection of increasingly high-dimensional neural data-sets. Making sense of such data requires new statistical methods for extracting shared latent structure underlying multi-neuron responses. Factor models provide one popular approach to this problem [1–5]. These models seek to characterize the structure underlying neural data in terms of a small number of latent variables. However, factor models can be cumbersome to learn when the prior distribution over the latent variables and the likelihood governing the observations are non-conjugate. This arises commonly for neural data, where binned spiking observations are best characterized by count models (e.g., binomial, Poisson, and negative-binomial).

Formally, latent factor models seek to explain shared structure underlying high-dimensional observations $(\mathbf{y}_1, \mathbf{y}_2, \dots, \mathbf{y}_T) \in \mathbb{R}^{N \times T}$ in terms of low-dimensional latent variables $(\mathbf{x}_1, \mathbf{x}_2, \dots, \mathbf{x}_T) \in \mathbb{R}^{P \times T}$, where $N > P$ and the observations are ordered sequentially in time from $t = 1$ to $t = T$. A popular approach is to model the time series of latent variables with a Gaussian process (GP), which makes few assumptions about latent trajectories beyond the fact that they evolve smoothly in time. When combined with a Gaussian observations model, the resulting approach is known as Gaussian Process Factor Analysis (GPFA) [1]. Recent work has extended GPFA to incorporate Poisson observations, which provides a more appropriate model for spike train data [5–8]. However, closed-form inference under GPFA models is only possible when the model likelihood and prior are conjugate. Consequently, Poisson and other non-conjugate models require approximations to fit hyperparameters or obtain parametric expressions for the posterior distribution over latents.

Here, we introduce a novel procedure for learning non-conjugate GPFA models with count observations, which we refer to as Polynomial Approximate Log-likelihood (PAL). This method exploits an idea for rapid inference in generalized linear models using so-called “approximate sufficient statistics” [9, 10], and extends it to the latent variable model setting. The basic idea involves approximating the nonlinear terms in the model log-likelihood using orthogonal polynomials. When the polynomial approximation is second-order, the likelihood term can be explicitly marginalized to obtain a closed-form expression for the marginal likelihood (the probability of the data given the parameters), and an approximately Gaussian posterior distribution over the latents. We explicitly derive PAL estimators for GPFA models with binomial, Poisson, and negative-binomial observation models.

We compare our approach to Black Box Variational Inference (BBVI), a state-of-the-art method for approximate inference in non-conjugate models that is renowned for its simplicity and adaptability [4, 11, 12]. Although BBVI can achieve higher accuracy in some cases, PAL compares favorably to BBVI in that it provides a closed-form expression for marginal likelihood that can be optimized directly; it therefore requires no careful tuning of learning rates, number of Monte Carlo samples, or stopping criteria, and does not suffer from high-variance estimates due to sampling-based evaluation of marginal likelihood. Moreover, PAL can be used to improve BBVI by providing a good initialization for the latents variables and hyperparameters. We show that PAL-based initialization speeds up and stabilizes the sampling-based optimization, offering a significant improvement over random initialization of BBVI.

We evaluate the performance of our methods by applying PAL and BBVI to two different multi-neuron datasets, one from mouse visual cortex and one from monkey parietal cortex, under three different choices of count model (binomial, Poisson, and negative binomial). We show that PAL achieves a substantial speedup over BBVI, and that count-GPFA models generally outperform standard Gaussian GPFA for extracting latent structure from spike train data. The PAL approach therefore offers a promising avenue for future work on non-conjugate models that arise frequently in the analysis of biological and other data.

2 Count-GPFA models

Consider a dataset consisting of count observations from N neurons over T time bins, $\mathbf{Y} \in \mathbb{N}^{N \times T}$. The count-GPFA model seeks to describe these data in terms of a nonlinearly transformed linear projection of lower-dimensional latent variable $\mathbf{X} \in \mathbb{R}^{P \times T}$, $P < N$, where each each latent variable evolves according to an independent Gaussian process. Thus the timecourse of the j 'th latent variable, which forms the j 'th row of \mathbf{X} , has a multivariate normal distribution:

$$\mathbf{x}_j \sim \mathcal{N}(0, K), \tag{1}$$

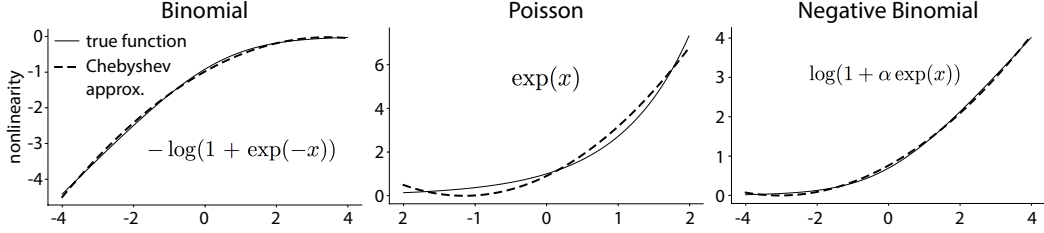


Figure 1: Comparison of second-order Chebyshev approximation to the nonlinear term found in the log-likelihood of binomial, Poisson, and negative-Binomial count-observation models for GPFA.

where \mathbf{K} is a $T \times T$ covariance matrix whose (t, t') 'th entry is given by the covariance function $k(t, t')$. In this paper, we use the common Gaussian or ‘‘squared exponential’’ covariance function: $k(t, t') = \exp(-(t - t')^2 / (2\ell^2))$, which is governed by a single hyperparameter, the ‘‘length scale’’ ℓ , which controls smoothness of the latent process.

The count-GPFA observation model can then be written:

$$\mathbf{Y}|\mathbf{W}, \mathbf{X} \sim \mathcal{P}(f(\mathbf{W}\mathbf{X})) \quad (2)$$

where $\mathbf{W} \in \mathbb{R}^{N \times P}$ is a loading matrix, $f(\cdot)$ denotes a nonlinear function that transforms $\mathbf{W}\mathbf{X}$ to the appropriate range for a count random variable (e.g., the non-negative reals), and \mathcal{P} denotes a probability distribution for count data.

Fitting the count-GPFA model to data involves inferring the loading weights \mathbf{W} and hyperparameters $\theta = \{\ell\}$ via numerical optimization of the marginal likelihood:

$$P(\mathbf{Y}|\mathbf{W}, \theta) = \int P(\mathbf{Y}|\mathbf{W}, \mathbf{X})P(\mathbf{X}|\theta)d\mathbf{X}. \quad (3)$$

However, non-conjugacy of the count model likelihood $P(\mathbf{Y}|\mathbf{W}, \mathbf{X})$ and Gaussian prior over latents $P(\mathbf{X}|\theta)$ means that this integral cannot be computed in closed form. Likewise, the posterior distribution over latents given the data, given by: $P(\mathbf{X}|\mathbf{Y}, \mathbf{W}, \theta) \propto P(\mathbf{Y}|\mathbf{X}, \mathbf{W})P(\mathbf{X}|\theta)/P(\mathbf{Y}|\mathbf{W}, \theta)$, has no closed form expression, where the desired normalizing constant is the marginal likelihood. Fitting and inference therefore rely on approximate inference methods.

3 Polynomial Approximate Log-likelihood (PAL)

Here we propose Polynomial Approximate Log-likelihood (PAL), an approximation scheme for efficient learning and inference in non-conjugate Gaussian latent variable models. The core idea is to approximate terms in the observation model log-likelihood that are nonlinear in \mathbf{X} using orthogonal polynomials. Our approach is inspired by recent work on ‘‘polynomial approximate sufficient statistics’’ for generalized linear models (PASS-GLMs) [9, 10]. In that work, the \mathbf{X} were observed regressors, and the method provided so-called ‘‘approximate sufficient statistics’’ that could be computed with a single pass over the data.

Here, the \mathbf{X} are (unobserved) latent variables instead of regressors, and the goal of the approximation is efficient marginalization rather than a set of sufficient statistics. We consider second-order polynomial approximations to the log-likelihood, which allow for analytic marginalization over latents. PAL therefore enables closed-form evaluation of the approximate marginal likelihood, allowing efficient optimization of parameters and hyperparameters.

We derive PAL estimators for GPFA under three different non-conjugate observation models: binomial, Poisson, and negative binomial (NB). These models range from under-dispersed or ‘‘sub-Poisson’’ for binomial to overdispersed or ‘‘supra-Poisson’’ for NB, thus spanning the range of dispersion behaviors found in different brain areas [12–19].

All PAL count-GPFA models have the same general form for the approximate log marginal likelihood (log evidence):

$$\mathcal{E}(\mathbf{y}|\mathbf{W}, \theta) \approx \frac{1}{2} \log |\boldsymbol{\Sigma}| + \frac{1}{2} \boldsymbol{\mu}^\top \boldsymbol{\Sigma}^{-1} \boldsymbol{\mu} - \frac{1}{2} \log |\mathbf{K}|, \quad (4)$$

	binomial	Poisson	negative binomial
spike rate λ_{it}	$n_i \sigma(\mathbf{w}_i^\top \mathbf{x}_t)$	$\exp(\mathbf{w}_i^\top \mathbf{x}_t)$	$\exp(\mathbf{w}_i^\top \mathbf{x}_t)$
nonlinear term	$-\log(1 + e^{-x})$	e^x	$\log(1 + \alpha e^x)$
\mathbf{H}	$2\tilde{\mathbf{W}}^\top \text{diag}(\tilde{\mathbf{n}} \circ \mathbf{a}) \tilde{\mathbf{W}}$	$2\tilde{\mathbf{W}}^\top \text{diag}(\mathbf{a}) \tilde{\mathbf{W}}$	$2\tilde{\mathbf{W}}^\top \text{diag}((\alpha^{-1} + \mathbf{y}) \circ \mathbf{a}) \tilde{\mathbf{W}}$
posterior mean $\boldsymbol{\mu}$	$\boldsymbol{\Sigma} \tilde{\mathbf{W}}^\top (\mathbf{y} - \tilde{\mathbf{n}} - \tilde{\mathbf{n}} \circ \mathbf{b})$	$\boldsymbol{\Sigma} \tilde{\mathbf{W}}^\top (\mathbf{y} - \mathbf{b})$	$\boldsymbol{\Sigma} \tilde{\mathbf{W}}^\top (\mathbf{y} - \mathbf{y} \circ \mathbf{b} - \alpha^{-1} \mathbf{b})$

Table 1: Summary of PAL expressions for count-GPFA models. Top line gives the spike rate of neuron i at time t given the latent vector \mathbf{x}_t and loading weights \mathbf{w}_i for neuron i . Second line gives the nonlinear term of the log-likelihood that must be approximated under PAL. The third row, \mathbf{H} is defined by $\mathbf{H} = \boldsymbol{\Sigma}^{-1} - \mathbf{K}^{-1}$, which succinctly presents posterior covariances, and the fourth line $\boldsymbol{\mu}$ shows approximate posterior means.

where $\boldsymbol{\Sigma}$ denotes an approximate posterior covariance and $\boldsymbol{\mu}$ denotes an approximate posterior mean, and \mathbf{K} is the prior covariance over all latents (a block-diagonal matrix, with one block for each latent). The form of the first two terms varies across models, which we derive for three specific models below. See Table 1 for a summary of the results for all count-GPFA models. For clarity, we define $\mathbf{H} = \boldsymbol{\Sigma}^{-1} - \mathbf{K}^{-1}$ in this table to succinctly present approximate posterior covariances.

3.1 PAL for Poisson-GPFA

We begin with the Poisson observation model, which is the most common model for spike counts and a popular choice for latent variable models of spike train data [5, 8, 20]. For this model, spike count y given a spike rate parameter λ is distributed according to:

$$P(y|\lambda) = \frac{1}{y!} (\Delta \lambda)^y e^{-(\Delta \lambda)}, \quad (5)$$

where Δ is the time bin size (which we set here to 1, resulting in spike rates in units of spikes/bin). We use an exponential nonlinearity from latents to spike rates, so the vector of spike rates at time t is:

$$\boldsymbol{\lambda}_t = \exp(\mathbf{W} \mathbf{x}_t). \quad (6)$$

This choice of nonlinearity gives rise to a log-likelihood with a single nonlinear term, although other nonlinearities can be considered [10].

The Poisson log-likelihood for the entire dataset can be written conveniently in vector form as:

$$\mathcal{L}(\mathbf{y}, \mathbf{x} | \mathbf{W}) = \mathbf{y}^\top \tilde{\mathbf{W}} \mathbf{x} - \mathbf{1}^\top \exp(\tilde{\mathbf{W}} \mathbf{x}) + \text{const} \quad (7)$$

where $\mathbf{y} = \text{vec}(\mathbf{Y})$ is a $NT \times 1$ vector of concatenated spike count observations from all N neurons and T time bins, $\mathbf{x} = \text{vec}(\mathbf{X})$ is a $PT \times 1$ vector of concatenated latent vectors across P latent time series, $\tilde{\mathbf{W}} = \mathbf{W} \otimes \mathbf{I}_T$ is a $NT \times PT$ Kronecker-structured matrix, and $\mathbf{1}$ is a length- NT vector of ones.

The only nonlinear term in the log-likelihood is the exponential term $\exp(\tilde{\mathbf{W}} \mathbf{x})$. We therefore approximate the exponential function with a second-order polynomial:

$$\exp(x) \approx ax^2 + bx + c, \quad (8)$$

with coefficients a , b , and c given by a Chebyshev polynomial approximation to $\exp(x)$ over an interval $\psi = [x_0, x_1]$, which we set independently for each neuron [10, 21]. We use Chebyshev polynomials because they provide efficient near-minimax polynomial approximations [9]. Specifically, we computed the truncated Chebyshev expansion of the exponential $\exp(x) = \sum_{m=0}^2 \beta_m T_m$ where T_m is the degree- m Chebyshev polynomial of the first kind over $[x_0, x_1]$ and β_m are the expansion coefficients over that interval. The coefficients a , b , and c are given by collecting the terms to rewrite the expansion in the monomial basis.

We selected the interval $[x_0, x_1]$ independently for each neuron by computing the log of the mean firing rate of each neuron, $\log \lambda_i$. Since the nonlinearity is over the input $\mathbf{W} \mathbf{x}$, and the firing rate is $\lambda = \exp(\mathbf{W} \mathbf{x})$, we take the log of λ_i as we wish to center the nonlinear approximation at the center of the empirical neuronal rate to maximize accuracy. See Figure 1 as an example of a range centered at 0, corresponding to a simulated GP drawn with mean 0. We then chose the limits of the range to

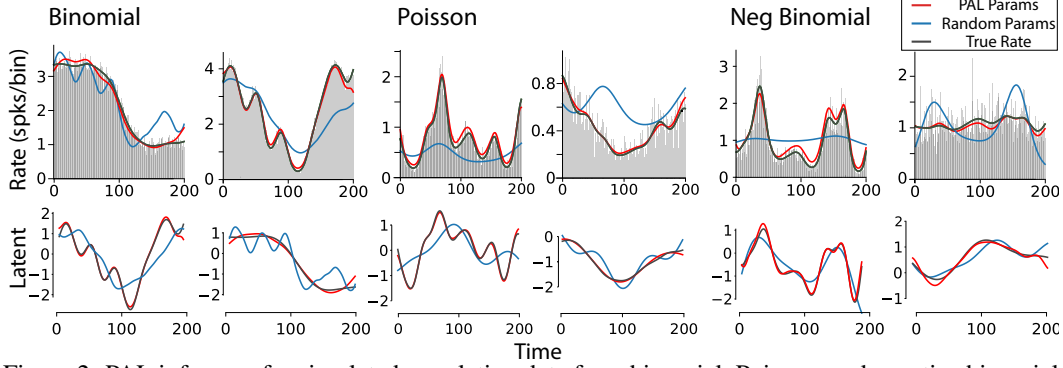


Figure 2: PAL inference for simulated population data from binomial, Poisson, and negative binomial GPFA models. Two example neurons (out of 20) are shown for each model. Top row: Inferred rate for neurons for PAL inference compared to a MAP estimate with randomly selected parameters. Two-dimensional latent trajectories recovered for each model (bottom).

be $[\log \lambda_i - 2, \log \lambda_i + 2]$, resulting in an approximation range extending from e^{-2} to e^2 times the mean firing rate. We found that this range balanced coverage in firing rate space with approximation accuracy. After selecting the range centers for each neuron, we computed the polynomial coefficients (a_i, b_i, c_i) for neuron i by gridding the interval of interest at a resolution of $dx = 0.01$ and solving for the coefficients that minimize the least squares between the true function and its polynomial approximation. For more detail, see [10].

Given coefficients for each neuron, the exponential term in the Poisson log-likelihood can be approximated:

$$\mathbf{1}^\top \exp(\tilde{\mathbf{W}}\mathbf{x}) \approx \sum_{t=1}^T \sum_{i=1}^N \left(a_i (\mathbf{W}\mathbf{x}_t)_i \circ (\mathbf{W}\mathbf{x}_t)_i + b_i (\mathbf{W}\mathbf{x}_t)_i + c_i \right) \quad (9)$$

$$= \mathbf{x}^\top \tilde{\mathbf{W}}^\top \text{diag}(\mathbf{a}) \tilde{\mathbf{W}}\mathbf{x} + \mathbf{b}^\top \tilde{\mathbf{W}}\mathbf{x} + \text{const} \quad (10)$$

where \circ denotes Hadamard (element-wise) multiplication, and the second line involves the concatenation of the polynomial coefficients for each neuron and time bin: $\mathbf{a} = [a_1 \mathbf{1}, \dots, a_n \mathbf{1}]^\top$, $\mathbf{b} = [b_1 \mathbf{1}, \dots, b_n \mathbf{1}]^\top$, and we can ignore the constants c_i .

We now substitute the polynomial approximation into the log-likelihood and add the log prior, giving:

$$\mathcal{L}(\mathbf{y}, \mathbf{x} | \tilde{\mathbf{W}}, \theta) \approx \mathbf{y}^\top \tilde{\mathbf{W}}\mathbf{x} - \mathbf{x}^\top \tilde{\mathbf{W}}^\top \text{diag}(\mathbf{a}) \tilde{\mathbf{W}}\mathbf{x} - \mathbf{b}^\top \tilde{\mathbf{W}}\mathbf{x} - \frac{1}{2} \mathbf{x}^\top \mathbf{K}^{-1} \mathbf{x} - \frac{1}{2} \log |\mathbf{K}|$$

Since this approximation is quadratic in \mathbf{x} we can exponentiate and then analytically marginalize \mathbf{x} to obtain an approximation to the log-likelihood that follows equation (4) where:

$$\Sigma^{-1} = 2\tilde{\mathbf{W}}^\top \text{diag}(\mathbf{a}) \tilde{\mathbf{W}} + \mathbf{K}^{-1} \quad (11)$$

$$\boldsymbol{\mu} = \Sigma \tilde{\mathbf{W}}^\top (\mathbf{y} - \mathbf{b}), \quad (12)$$

and we have dropped terms that do not depend on $\tilde{\mathbf{W}}$ or θ .

3.2 PAL for Binomial-GPFA

Deriving the PAL estimator for a binomial observation model follows a similar logic to the Poisson case. Recall that for binomial model, spike count y is distributed according to :

$$P(y|p, n) = \binom{n}{y} p^y (1-p)^{(n-y)}, \quad (13)$$

where p is the “probability of success” and n is the “number of trials” parameter. For this model, we map latents through a sigmoidal nonlinearity, $\sigma(x) = 1/(1 + \exp(-x))$, to obtain the binomial parameter p , and we set the number-of-trials parameter separately for each neuron using the maximum

number of observed spikes in a single time bin. The vector of spike rates at time t for this model is thus given by:

$$\boldsymbol{\lambda}_t = \mathbf{n} \circ \sigma(\mathbf{W}\mathbf{x}_t), \quad (14)$$

where $\mathbf{n} = (n_1, \dots, n_N)^\top$ is the vector of max-count parameters across neurons.

We can write the log-likelihood in vectorized form as:

$$\mathcal{L}(\mathbf{y}|\mathbf{x}, \tilde{\mathbf{W}}) = (-\tilde{\mathbf{n}} + \mathbf{y})^\top \tilde{\mathbf{W}}\mathbf{x} - \tilde{\mathbf{n}}^\top \log(1 + \exp(-\tilde{\mathbf{W}}\mathbf{x})) + \text{const} \quad (15)$$

where $\tilde{\mathbf{n}} = (n_1\mathbf{1}, \dots, n_N\mathbf{1})^\top$ is the concatenated vector of max-count parameters for each neuron across time bins, and we have ignored terms that do not depend on $\tilde{\mathbf{W}}\mathbf{x}$.

The problematic term here is the nonlinear second term, $\log(1 + \exp(-x))$, which we approximate, as before, using a second-order Chebyshev polynomial approximation. We use a range of $[-4, 4]$ for the Chebyshev approximation, consistent with previous work in the logistic regression case [9]. This results in an approximation to the log-likelihood of the form:

$$\mathcal{L}(\mathbf{y}|\mathbf{x}, \tilde{\mathbf{W}}) \approx -\mathbf{x}^\top \tilde{\mathbf{W}}^\top \text{diag}(\tilde{\mathbf{n}} \circ \mathbf{a}) \tilde{\mathbf{W}}\mathbf{x} + (\mathbf{y} - \tilde{\mathbf{n}} - \tilde{\mathbf{n}} \circ \mathbf{b})^\top \tilde{\mathbf{W}}\mathbf{x} + \text{const} \quad (16)$$

As in the Poisson case, we can add the log-prior to the above expression, exponentiate and marginalize over \mathbf{x} to obtain an approximation to the log marginal likelihood in the same form as equation (4). In this case, we obtain matrix and vector terms:

$$\boldsymbol{\Sigma}^{-1} = 2\tilde{\mathbf{W}}^\top \text{diag}(\tilde{\mathbf{n}} \circ \mathbf{a}) \tilde{\mathbf{W}} + \mathbf{K}^{-1} \quad (17)$$

$$\boldsymbol{\mu} = \boldsymbol{\Sigma} \tilde{\mathbf{W}}^\top (\mathbf{y} - \tilde{\mathbf{n}} - \tilde{\mathbf{n}} \circ \mathbf{b}). \quad (18)$$

3.3 PAL for negative-binomial GPFA

Lastly, we consider a negative binomial observation model, which covers the over-dispersed spike responses [16, 17, 22]. For negative-binomial GPFA, we use a non-standard parametrization of the negative binomial distribution in terms of mean parameter m , and scale parameter $r = 1/\alpha$:

$$P(y|m, \alpha) = \frac{\Gamma(y + \alpha^{-1})}{\Gamma(\alpha^{-1})\Gamma(y + 1)} \left(\frac{1}{1 + \alpha m}\right)^{\alpha^{-1}} \left(\frac{\alpha m}{1 + \alpha m}\right)^y \quad (19)$$

This form of the distribution maps to the standard negative-binomial distribution, $p(y|p, r) = \binom{y+r-1}{y} (1-p)^r p^y$, via $p = \frac{r}{m+r}$.

Parameterizing the negative binomial model this way makes for a simple expression of the expected spike count, which is equal to the model parameter m . Let us define this mean rate in the factor analytic framework as $m = \exp(\tilde{\mathbf{W}}\mathbf{x})$. This allows us to write the log-likelihood in vector form as:

$$\mathcal{L}(\mathbf{y}|\mathbf{W}, \mathbf{x}, \alpha) = \mathbf{y}^\top \tilde{\mathbf{W}}\mathbf{x} - (\alpha^{-1} + \mathbf{y}^\top) \log(1 + \alpha \exp(\tilde{\mathbf{W}}\mathbf{x})) + \text{const}. \quad (20)$$

To derive a PAL estimator, we use a quadratic approximation to the nonlinear term $\log(1 + \alpha \exp(x))$ on a per-neuron basis. We set $\alpha = 1$ for simulations, but this quantity may be learned in an outer loop. We choose the center of the nonlinear range to be the same as in the Poisson case, with the center value being the log of the mean firing rate of the neuron (see right panel of Figure 1 for example of centering with an average log-rate of 0). The range limits are $[\log \lambda_i - 4, \log \lambda_i + 4]$, where λ_i is the average value of m across time, per neuron. Here, a wider range can be used as this nonlinearity is accurately captured by the quadratic approximation. As in the previous cases, we obtain a quadratic approximate log-likelihood which has the following form:

$$\mathcal{L}(\mathbf{y}|\mathbf{x}, \tilde{\mathbf{W}}, \alpha) \approx -\mathbf{x}^\top \tilde{\mathbf{W}}^\top \text{diag}((\alpha^{-1} + \mathbf{y}) \circ \mathbf{a}) \tilde{\mathbf{W}}\mathbf{x} + (\mathbf{y} - \mathbf{y} \circ \mathbf{b} - \alpha^{-1}\mathbf{b})^\top \tilde{\mathbf{W}}\mathbf{x} + \text{const} \quad (21)$$

We then add the log prior and marginalize \mathbf{x} to obtain an approximation to the log marginal likelihood for negative-binomial GPFA that follows the same form as equation (4) with

$$\boldsymbol{\Sigma}^{-1} = 2\tilde{\mathbf{W}}^\top \text{diag}((\alpha^{-1} + \mathbf{y}) \circ \mathbf{a}) \tilde{\mathbf{W}} + \mathbf{K}^{-1} \quad (22)$$

$$\boldsymbol{\mu} = \boldsymbol{\Sigma} \tilde{\mathbf{W}}^\top (\mathbf{y} - \mathbf{y} \circ \mathbf{b} - \alpha^{-1}\mathbf{b}) \quad (23)$$

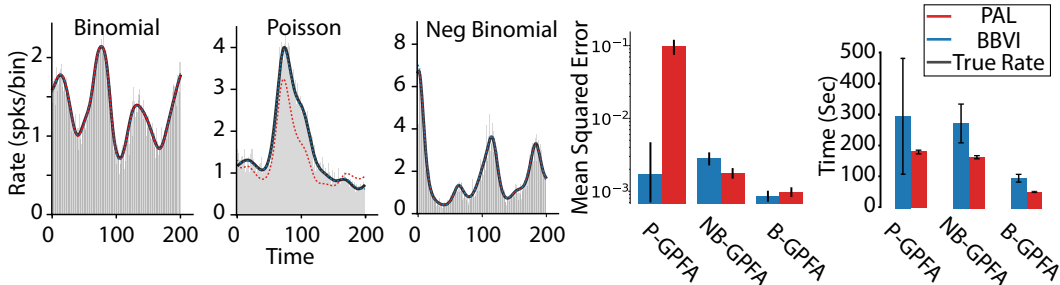


Figure 3: Comparison of BBVI and PAL-based estimation for inference in count-GPFA models. **(Left)** MAP estimation of the latents yields reconstructions conditioned on PAL-learned hyperparameters (red) and full BBVI (blue). PAL reconstruction for Binomial and negative-Binomial GPFA are highly accurate, but for Poisson can be off by a scale factor for certain neurons. **(Right)** PAL estimation procedure computation time compared to BBVI time for ten runs of Poisson GPFA inference.

3.4 Evaluating PAL performance

To assess the accuracy of the PAL estimator, we first analyzed its performance on simulated data. For 20 trials with 200 time points, we simulated count observations from 20 neurons with 2 latent variables with $\ell_1 = 15$, $\ell_2 = 60$ and each entry of \mathbf{W} drawn uniformly in $[0,2]$. The PAL method provides accurate latent variable recovery as demonstrated by the reconstructions shown in Figure 2. Here, we directly optimized equation 4 for all models to find optimal parameters \mathbf{W} and hyperparameters ℓ , and then maximized the conditional posterior to identify \mathbf{X} (MAP estimate). As a control, our random parameters were given by a new random draw for \mathbf{W} , and ℓ drawn uniformly in $[10,100]$.

We found that the rates estimated using this procedure were similar to the true model rates and showed substantial improvement above random parameter selection (Figure 2). Additionally, PAL inference accurately captures latent structure (Figure 2, bottom). To identify latent structure in these simulated data, we regress learned latents onto the true latents as latent factors models are identifiable only up to a rotation matrix. Accurate identification of latent structure is a primary feature of this inference procedure, as latents have functional importance in neuroscience settings [1, 8].

A summary of the features of all count model GPFA is given in Table 1. Here, we show the non-linearities approximated by Chebyshev polynomials for each model, the expected number of spikes for the i th neuron as a function of the latents, \mathbf{X} , and loadings matrix \mathbf{W} , and the variance and mean of the polynomial-approximated marginal distribution. Here, n_i corresponds to the maximum number of spikes observed in a single time-bin for neuron i , and \mathbf{w}_i refers to the i th column of \mathbf{W} .

4 Black-Box Variational Inference

Variational inference represents a common alternate approach to performing inference in non-conjugate factor models, and has been previously used in the setting of Poisson-GPFA [8, 20]. Recall that variational inference seeks to maximize an evidence lower bound (ELBO) using a variational distribution $q_\phi(\mathbf{X})$ parameterized by ϕ in place of the posterior [23]

$$\mathcal{F}(\theta, \phi) = -D_{KL}(q_\phi(\mathbf{X})|p_\theta(\mathbf{X})) + \mathbb{E}_{q_\phi}[\log(p_\theta(\mathbf{y}|\mathbf{X}, \mathbf{W}))]. \quad (24)$$

We optimize the model and variational parameters using samples from $q_\phi(X)$. To reduce variance, we parameterized $q_\phi(X)$ as a differentiable function of standard normal random variables $f(\epsilon, \phi)$ and computed gradients with respect to ϕ using the local reparameterization trick [24].

Controlling the variance of stochastic gradients of the ELBO in BBVI is an active area of research. The use of sampling in the optimization poses considerable challenges in convergence, and as such a variety of techniques have been introduced to reduce variance in the gradient estimates, including use of a natural gradient for optimization [25, 26], reformulating the gradient estimator [27], and the reparameterization trick [24, 28]. Despite employing the reparameterization trick, we have likewise found for our GP latent models that BBVI is similarly unstable and can take widely variable amounts of time to converge depending on initialization of the parameters and the stochastic trajectory (Figure 3). Further, we use Adam optimization [29], which will occasionally find local maxima and retain a

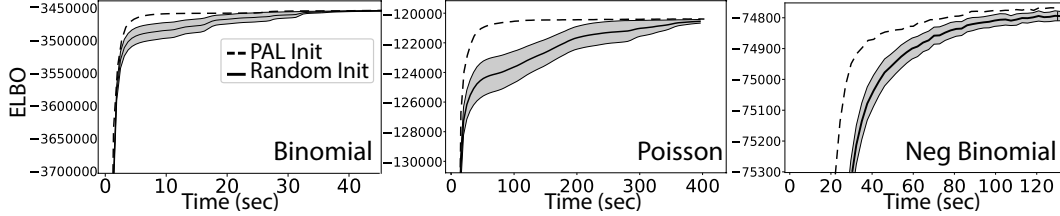


Figure 4: Optimization time for full BBVI from either a random initialization or PAL initialization for all count-GPFA models. Data is shown as mean and standard error for 10 trajectories.

low value of the ELBO estimate for a substantial period of time. Despite these shortcomings, we have found that if the sampling-based inference is allowed to run for long enough, BBVI recovers true latent structure.

We employ BBVI on our count-GPFA models and compare performance to PAL. Though PAL and BBVI tend to converge to a highly accurate solution for Binomial and Negative Binomial GPFA, in settings where the PAL nonlinearity is not well approximated by a quadratic function (1), BBVI performance is often better than PAL inference. For our models, this is true in the Poisson case, where the nonlinearity (\exp) is most difficult to capture. We show an example of this in Figure 3, where BBVI has higher performance capturing neuronal tuning than the PAL inference procedure. The scaling factor for these neurons' rates is sometimes off, and here a poorly reconstructed neuron is chosen for illustration. Often, many of the neurons for P-GPFA are well captured (as in Figure 2), but occasionally a few neurons are off by such a scale factor. Average MSE across all neurons for all count GPFA models are shown in the middle panel of Figure 3, showing PALs limitations in the Poisson case with an exponential nonlinearity. However, even in this case, times-to-convergence are faster and much more stable using the PAL approach. This is demonstrated on the right panel of Figure 3 for all count-GPFA models. The time to converge for PAL optimization is faster and less variable than full BBVI optimization, as evidenced by the average times-to-convergence of ten runs of each optimization procedure. In the BBVI case, convergence was determined when the ELBO was within 99.9% of the maximal ELBO value identified. For occasional BBVI runs for each count model, this value was not achieved for the duration of the inference procedure, as the the ELBO was stuck at a local maxima. These convergence times were discarded when calculating the mean convergence time, and demonstrative of the irregularity of the BBVI inference procedure. Conversely, the PAL hyperparameter identification followed by a MAP estimation is a fast and reliable inference procedure with limited variability in inference time and a sensible convergence end-point.

4.1 PAL hyperparameter identification as initialization for BBVI

For use in these situations where the PAL approximation does not accurately capture likelihood nonlinearities, we can combine PAL and BBVI methods to provide a robust and reliable inference procedure. We do this by initializing the BBVI algorithm with the hyperparameters provided by optimization of equation 4. This procedure is more stable than full BBVI with random initial hyperparameters, and achieves accurate model recovery. We demonstrate this is true not just for Poisson-GPFA, where BBVI ultimately provides more-accurate solutions, but extends to all count-GPFA models. Figure 4 shows the evolution of the ELBO in time during optimization for all models. In each case, BBVI is run 10 times, either initializing randomly or initializing at the PAL-optimal hyperparameters. Standard error is shown in grey for the random initialization, but not shown for PAL-initialized optimization, as this trajectory follows nearly identically for each run. An initial sharp increase in the ELBO is always observed in all models, as here latent structure is approximately identified, but hyperparameters are tuned at the end of the BBVI optimization procedure. Here, we have cut off the initial rise in ELBO for clarity. Figure 4 thus demonstrates the end of the optimization procedure, where randomly initialized BBVI attempts to find hyperparameters along varying trajectories. For this random initialization, finding hyperparameters poses a challenge in this final portion of inference, yielding variable paths to the true maximum ELBO, and an uncertainty surrounding when the maximum has been achieved. This is despite using state-of-the-art methods for BBVI inference [24, 29]. In fact, for many of the trajectories tested, the optimum ELBO value was not within 99.9% of the maximum value seen using PAL-initialization for the entire duration of the time ran. This suggests that the BBVI inference approach is uncertain, and it can be impossible to tell

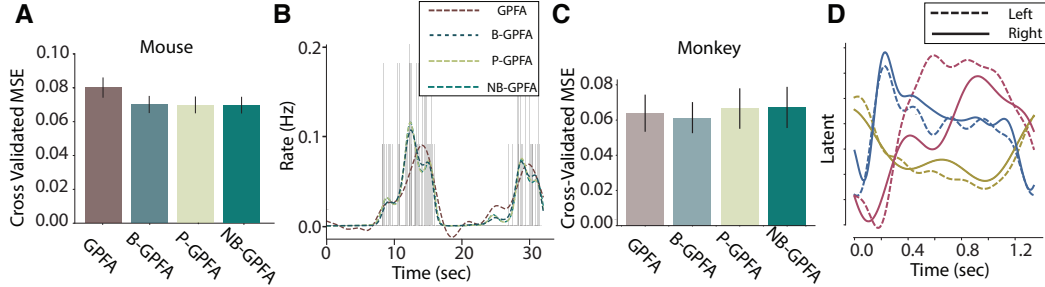


Figure 5: Average mean squared error (MSE) on hold-out trials for all GPFA models for mouse (A) and monkey (C) data. Average reconstructed neural rates for all count-GPFA models for an example rodent neuron (B). Latents regressed to the same subspace for different choice conditions for monkey data (D).

when the procedure has achieved a true maximum, or is stuck in a local optimum. PAL-initialization overcomes this limitation, and though the combination of procedures may not offer a significant time speed up, our polynomial approximation provides a principled method to initialize BBVI. This suggests a useful approach in future methods in managing sampling-based variational inference.

5 Application of count GPFA models to Neural Data

We use our count-GPFA inference procedure to compare GPFA models with different noise characterizations to see which latent variable model best describes observed spiking data. We test these models on two data sets, one from monkey parietal and high-level visual cortices, and the other from rodent V1. For the monkey data, 14 neurons were recorded from the middle temporal visual (MT) and lateral intraparietal (LIP) areas across 100 1.4-second trials of a visual perceptual decision-making task [30]. In this task, the animal accumulates visual evidence towards left or right targets (choices). For our rodent data, spike times from 49 neurons recorded during passive viewing 20 repeated 32-second trials of a gratings stimulus. The stimulus has 8 orientations at fixed spatial and temporal frequencies. Stimuli are presented for 4 seconds each.

For the rodent data, the estimated latent dimensionality was 6 for all count-GPFA models, chosen via maximization of cross-validated log-likelihood. Count-GPFA models exhibited best cross-validation error for the rodent data, with GPFA exhibiting worse performance (Figure 5A). Cross-validation error was measured by mean-squared error of predicted neuronal firing to a smoothed PSTH, averaged across neurons. The differences in performance of count-GPFA predictions of neural rates are demonstrated in Figure 5B. Here, the GPFA predictions are often negative, an impossibility with count-GPFA models. Additionally, GPFA overestimates smoothness of neural trajectories, attributing neural variability to observation noise rather than changes in rates. Count-GPFA models better capture situations where data are low-rate and involve abrupt changes in spiking.

For the monkey data, latent dimensionality for these data was selected to be 3 dimensional for all models tested, verified again by cross validated log-likelihood. Mean squared error was calculated and reported as it was for the rodent data. For these data, all GPFA models exhibited equal performance on cross-validation (Figure 5C), with a small bias favoring Binomial-GPFA. The differences in performance here are likely due to the data being higher-rate, fewer neurons, and more trials.

Count-GPFA models can find meaningful latent structure in neural data. For our monkey data, we fit the models separately to the trials with left and right choices. We visualized the inferred latent variables from the Binomial GPFA model with 3 latent dimensions for these two sets of trials. To perform a meaningful comparison of the latents across the two models, we linearly transformed the loading matrices to approximately span the same subspace. We then transformed the corresponding latents with the inverse of this transformation. The latents for the two conditions are shown in (Figure 5D). Two of the latents are closely overlapping, which suggests the presence of shared structure across the two conditions. Interestingly, one latent (red) diverges near 400ms after trial onset, which falls into the portion of the trial where the animal is putatively making its choice. This suggests that

this latent may encode the choice variable in these neural data, and is a promising future direction of further exploration for count-GPFA models.

6 Conclusion

We have developed a novel technique for learning count Gaussian process factor analytic models that uses a polynomial approximate log-likelihood (PAL) for rapid closed-form evaluation of marginal likelihoods. This approximation can be used to estimate model parameters directly, or to provide initial values for black box variational inference that overcomes significant well-known BBVI optimization limitations. These inference methods achieve high accuracy extracting low dimensional latent structure from simulated spike train data. We tested our various non-conjugate GPFA models on neural data and these count-GPFA models are comparable or better than traditional GPFA approaches, which do not often consider count noise.

References

- [1] BM Yu, JP Cunningham, G Santhanam, SI Ryu, KV Shenoy, and M Sahani. Gaussian-process factor analysis for low-dimensional single-trial analysis of neural population activity. In *Adv neur inf proc sys*, pages 1881–1888, 2009.
- [2] John P Cunningham and B M Yu. Dimensionality reduction for large-scale neural recordings. *Nature neuroscience*, 17(11):1500–1509, 2014.
- [3] KC Lakshmanan, PT Sadtler, EC Tyler-Kabara, AP Batista, and BM Yu. Extracting low-dimensional latent structure from time series in the presence of delays. *Neural computation*, 2015.
- [4] Evan Archer, Il Memming Park, Lars Buesing, John Cunningham, and Liam Paninski. Black box variational inference for state space models. *stat*, 1050:23, 2015.
- [5] Anqi Wu, Nicholas G Roy, Stephen Keeley, and Jonathan W Pillow. Gaussian process based nonlinear latent structure discovery in multivariate spike train data. In I. Guyon, U. V. Luxburg, S. Bengio, H. Wallach, R. Fergus, S. Vishwanathan, and R. Garnett, editors, *Advances in Neural Information Processing Systems 30*, pages 3499–3508. Curran Associates, Inc., 2017.
- [6] L Buesing, J H Macke, and M Sahani. Spectral learning of linear dynamics from generalised-linear observations with application to neural population data. In *Adv neur inf proc sys*, pages 1682–1690, 2012.
- [7] Jakob H Macke, Lars Buesing, John P Cunningham, M Yu Byron, Krishna V Shenoy, and Maneesh Sahani. Empirical models of spiking in neural populations. In *Advances in neural information processing systems*, pages 1350–1358, 2011.
- [8] Yuan Zhao and Il Memming Park. Variational latent gaussian process for recovering single-trial dynamics from population spike trains. *Neural computation*, 29(5):1293–1316, 2017.
- [9] Jonathan Huggins, Ryan P Adams, and Tamara Broderick. Pass-glm: polynomial approximate sufficient statistics for scalable bayesian glm inference. In *Advances in Neural Information Processing Systems*, pages 3614–3624, 2017.
- [10] David M Zoltowski and Jonathan W Pillow. Scaling the poisson glm to massive neural datasets through polynomial approximations. In S. Bengio, H. Wallach, H. Larochelle, K. Grauman, N. Cesa-Bianchi, and R. Garnett, editors, *Advances in Neural Information Processing Systems 31*, pages 3521–3531. Curran Associates, Inc., 2018.
- [11] Rajesh Ranganath, Sean Gerrish, and David Blei. Black box variational inference. In *Artificial Intelligence and Statistics*, pages 814–822, 2014.
- [12] Yuanjun Gao, Lars Busing, Krishna V Shenoy, and John P Cunningham. High-dimensional neural spike train analysis with generalized count linear dynamical systems. In *Advances in neural information processing systems*, pages 2044–2052, 2015.
- [13] M. Shadlen and W. Newsome. The variable discharge of cortical neurons: implications for connectivity, computation, and information coding. *Journal of Neuroscience*, 18:3870–3896, 1998.
- [14] P. Kara, P. Reinagel, and R. C Reid. Low response variability in simultaneously recorded retinal, thalamic, and cortical neurons. *Neuron*, 27:636–646, 2000.

- [15] Gaby Maimon and John A Assad. Beyond poisson: increased spike-time regularity across primate parietal cortex. *Neuron*, 62(3):426–440, May 2009.
- [16] Jonathan Pillow and James Scott. Fully bayesian inference for neural models with negative-binomial spiking. In P. Bartlett, F.C.N. Pereira, C.J.C. Burges, L. Bottou, and K.Q. Weinberger, editors, *Advances in Neural Information Processing Systems 25*, pages 1907–1915, 2012.
- [17] RLT Goris, JA Movshon, and EP Simoncelli. Partitioning neuronal variability. *Nature neuroscience*, 17(6):858–865, 2014.
- [18] Ian H Stevenson. Flexible models for spike count data with both over-and under-dispersion. *Journal of computational neuroscience*, 41(1):29–43, 2016.
- [19] Adam S Charles, Mijung Park, J Patrick Weller, Gregory D Horwitz, and Jonathan W Pillow. Dethroning the fano factor: A flexible, model-based approach to partitioning neural variability. *Neural computation*, 30(4):1012–1045, 2018.
- [20] Lea Duncker and Maneesh Sahani. Temporal alignment and latent gaussian process factor inference in population spike trains. *bioRxiv*, page 331751, 2018.
- [21] John C Mason and David C Handscomb. *Chebyshev polynomials*. CRC Press, 2002.
- [22] Scott Linderman, Ryan P Adams, and Jonathan W Pillow. Bayesian latent structure discovery from multi-neuron recordings. In *Advances in neural information processing systems*, pages 2002–2010, 2016.
- [23] David M Blei, Andrew Y Ng, and Michael I Jordan. Latent dirichlet allocation. *Journal of machine Learning research*, 3(Jan):993–1022, 2003.
- [24] Diederik P Kingma, Tim Salimans, and Max Welling. Variational dropout and the local reparameterization trick. In *Advances in Neural Information Processing Systems*, pages 2575–2583, 2015.
- [25] Matthew D Hoffman, David M Blei, Chong Wang, and John Paisley. Stochastic variational inference. *The Journal of Machine Learning Research*, 14(1):1303–1347, 2013.
- [26] Hugh Salimbeni, Stefanos Eleftheriadis, and James Hensman. Natural gradients in practice: Non-conjugate variational inference in gaussian process models. *arXiv preprint arXiv:1803.09151*, 2018.
- [27] Geoffrey Roeder, Yuhuai Wu, and David Duvenaud. Sticking the landing: An asymptotically zero-variance gradient estimator for variational inference. *Advances in Neural Information Processing Systems*, 2017.
- [28] Danilo Jimenez Rezende, Shakir Mohamed, and Daan Wierstra. Stochastic backpropagation and approximate inference in deep generative models. *arXiv preprint arXiv:1401.4082*, 2014.
- [29] Diederik P Kingma and Jimmy Ba. Adam: A method for stochastic optimization. *arXiv preprint arXiv:1412.6980*, 2014.
- [30] Jacob L Yates, Il Memming Park, Leor N Katz, Jonathan W Pillow, and Alexander C Huk. Functional dissection of signal and noise in mt and lip during decision-making. *Nature neuroscience*, 20(9):1285, 2017.